

Genome-wide association study identifies a psoriasis susceptibility locus at *TRAF3IP2*

Eva Ellinghaus¹, David Ellinghaus¹, Philip E Stuart², Rajan P Nair², Sophie Debrus³, John V Raelson³, Majid Belouchi³, H el ene Fournier³, Claudia Reinhard³, Jun Ding⁴, Yun Li⁴, Trilokraj Tejasvi², Johann Gudjonsson², Stefan W Stoll², John J Voorhees², Sylviane Lambert², Stephan Weidinger^{5,6}, Bernadette Eberlein⁵, Manfred Kunz⁷, Proton Rahman⁸, Dafna D Gladman⁹, Christian Gieger¹⁰, H Erich Wichmann¹⁰⁻¹², Tom H Karlsen¹³, Gabriele Mayr¹⁴, Mario Albrecht¹⁴, Dieter Kabelitz¹⁵, Ulrich Mrowietz⁶, Gonalo R Abecasis⁴, James T Elder^{2,16}, Stefan Schreiber¹, Michael Weichenthal^{6,17} & Andre Franke^{1,17}

Psoriasis is a multifactorial skin disease characterized by epidermal hyperproliferation and chronic inflammation, the most common form of which is psoriasis vulgaris (PsV). We present a genome-wide association analysis of 2,339,118 SNPs in 472 PsV cases and 1,146 controls from Germany, with follow-up of the 147 most significant SNPs in 2,746 PsV cases and 4,140 controls from three independent replication panels. We identified an association at *TRAF3IP2* on 6q21 and genotyped two SNPs at this locus in two additional replication panels (the combined discovery and replication panels consisted of 6,487 cases and 8,037 controls; combined $P = 2.36 \times 10^{-10}$ for rs13210247 and combined $P = 1.24 \times 10^{-16}$ for rs33980500). About 15% of psoriasis cases develop psoriatic arthritis (PsA). A stratified analysis of our datasets including only PsA cases (1,922 cases compared to 8,037 controls, $P = 4.57 \times 10^{-12}$ for rs33980500) suggested that *TRAF3IP2* represents a shared susceptibility for PsV and PsA. *TRAF3IP2* encodes a protein involved in IL-17 signaling and which interacts with members of the Rel/NF- κ B transcription factor family.

Psoriasis (MIM177900) is a chronic immune-mediated and hyperproliferative disorder of the skin that affects up to 3% of individuals in populations of European ancestry¹⁻³. The most common form, PsV, is characterized by red, raised, scaly plaques that commonly occur on the elbows, knees, scalp and lower back⁴.

Disease concordance in monozygotic twin pairs amounts to at most 70% (ref. 5), and the sibling recurrence risk, λ_s , of PsV has been estimated to range between 4 and 11 (refs. 5,6). Part of the genetic

susceptibility can be explained by the established susceptibility locus at *PSORS1* in the human leukocyte antigen (HLA) complex on chromosome 6p21.3 (*HLA-C*) as well as polymorphisms at the *IL12B* (ref. 7), *IL23R* (refs. 8-11), *IL4-IL13* (ref. 12), *IL23A*, *TNIP1* and *TNFAIP3* (ref. 13) loci. Because these susceptibility loci only account for a λ_s of less than 1.35 (ref. 13), a large fraction of the heritability for PsV remains unexplained. In addition, a deletion of two *LCE* cluster genes has been proposed to be a risk factor for the development of psoriasis, implying that structural variants could also contribute to overall disease susceptibility¹⁴.

To identify additional PsV susceptibility loci, we performed genome-wide SNP genotyping of 487 German PsV cases and 1,161 controls (screening panel A; **Supplementary Table 1**) using the Illumina HumanHap 550K array. For genotype imputation with phased HapMap data as a reference and for subsequent statistical analysis, we used a dataset that passed stringent quality control filters. This cleaned dataset consisted of 504,742 autosomal SNPs genotyped in 472 cases and 1,146 controls. Imputation served to considerably increase the genomic coverage of our study to a total number of 2,339,118 SNPs. Conservatively accounting for multiple testing by Bonferroni correction, the threshold for genome-wide significance was $P \leq 2.14 \times 10^{-8}$ in the imputed dataset. A moderate genomic control value of $\lambda_{GC} = 1.065$ indicated a minimal overall inflation of the test statistics due to population stratification. Furthermore, the multidimensional scaling analysis showed genuine European ancestry of panel A samples, and identity-by-state analysis revealed neither non-European outliers nor cryptically related individuals after quality control screening (**Supplementary Fig. 1**). Our screening panel A

¹Institute of Clinical Molecular Biology, Christian-Albrechts-University, Kiel, Germany. ²Department of Dermatology, University of Michigan, Ann Arbor, Michigan, USA. ³Genizon BioSciences, Inc., St. Laurent, Quebec, Canada. ⁴Department of Biostatistics, Center for Statistical Genetics, University of Michigan, Ann Arbor, Michigan, USA. ⁵Department of Dermatology and Allergy, Technische Universit at M unchen, Munich, Germany. ⁶Department of Dermatology, University Hospital Schleswig-Holstein, Christian-Albrechts-University, Kiel, Germany. ⁷Comprehensive Center for Inflammation Medicine, University of L ubeck, L ubeck, Germany. ⁸Department of Medicine, Memorial University, St. John's, Newfoundland, Canada. ⁹Division of Rheumatology, University of Toronto, Psoriatic Arthritis Program, University Health Network, Toronto, Ontario, Canada. ¹⁰Institute of Epidemiology, Helmholtz Centre Munich, German Research Center for Environmental Health, Neuherberg, Germany. ¹¹Institute of Medical Informatics, Biometry and Epidemiology, Ludwig-Maximilians-University, Munich, Germany. ¹²Klinikum Grosshadern, Munich, Germany. ¹³Clinic for Specialized Medicine and Surgery, Oslo University Hospital Rikshospitalet, Oslo, Norway. ¹⁴Max Planck Institute for Informatics, Saarbr ucken, Germany. ¹⁵Institute for Immunology, University Hospital Schleswig-Holstein, Christian-Albrechts-University, Kiel, Germany. ¹⁶Ann Arbor Veterans Affairs Hospital, Ann Arbor, Michigan, USA. ¹⁷These authors contributed equally to this work. Correspondence should be addressed to A.F. (a.franke@muco.de) or M.W. (mweichenthal@dermatology.uni-kiel.de).

Received 25 February; accepted 26 July; published online 17 October 2010; doi:10.1038/ng.689



had 80% power to detect a variant with an odds ratio of 1.38 or higher at the 5% significance level, assuming a frequency of the disease-associated allele of at least 30% in controls.

The initial comparison of case-control frequencies confirmed the association of PsV with the established susceptibility loci at *HLA-C* (rs12191877, $P = 4.21 \times 10^{-32}$, odds ratio (OR) = 2.79, 95% CI 2.35–3.33) and *IL12B* (rs2546890, $P = 8.83 \times 10^{-8}$, OR = 0.65, 95% CI 0.56–0.76). Suggestive evidence for association was found for *IL23R* (rs1004819, $P = 6.17 \times 10^{-4}$, OR = 1.33, 95% CI 1.13–1.57) and on 1q21 22 kb upstream of *LCE3C* (rs4112788, $P = 6.36 \times 10^{-4}$, OR = 0.76, 95% CI 0.64–0.89) (Supplementary Fig. 2). The lead SNPs rs2546890 and rs1004819 were in moderate linkage disequilibrium (LD) ($r^2 > 0.50$) with the previously described associated variants at the *IL12B* (rs7709212)^{9,15} and *IL23R* (rs2201841)¹³ loci, respectively.

To identify additional susceptibility loci, we excluded all SNPs within the extended HLA complex (chromosome 6p21 at 25–34 Mb) and visually inspected the cluster plots of all genotyped index SNPs with a P value less than 0.001 after the clumping procedure. The 180 most strongly associated SNPs were subsequently selected for replication analysis and genotyped in the German replication panel B (681 cases and 1,824 controls). After quality control, we excluded 33 follow-up SNPs.

In addition, an *in silico* replication was performed using available genome-wide association study (GWAS) datasets for panel C from the United States (1,303 cases and 1,322 controls; Collaborative Association Study of Psoriasis (CASP))¹³ and for panel D from Canada (762 cases and 994 controls; S.D., J.V.R., M.B., H.F. and C.R., unpublished data). We imputed both datasets, that is, the CASP dataset, which was genotyped by Perlegen Sciences, and the Canadian dataset, which was generated using the Illumina Human 1M BeadChip. Of the 147 SNPs genotyped in panel B, we obtained genotypes for 126 SNPs in panel C and for 144 SNPs in panel D. Detailed association results including genotype counts of the 147 SNPs are given in Supplementary Table 2.

Two SNPs upstream of *IL12B*, included as a positive control for our experiment, achieved genome-wide significance in the combined replication panels B through D (rs2546890: replication stage $P = 9.07 \times 10^{-15}$; rs953861: replication stage $P = 6.50 \times 10^{-14}$). A previously unidentified association in the combined analysis of the three replication panels was obtained for rs13210247 (replication stage $P = 6.25 \times 10^{-6}$, risk allele frequency for cases = 0.09, risk allele frequency for controls = 0.07) with association robust to Bonferroni correction (corrected significance threshold of $\alpha = 3.4 \times 10^{-4}$, calculated as $0.05/147$). This intronic SNP is located in *TRAF3IP2*, which encodes the TRAF3 interacting protein 2 and which is also known as *ACT1*, encoding the NF- κ B activator 1 protein. In the combined panels A through D, consisting of a total of 3,218 PsV cases and 5,286 controls, this SNP achieved genome-wide significance (combined $P = 7.31 \times 10^{-9}$) (Fig. 1). We observed suggestive evidence for association for four other SNPs; however, these associations did not remain significant after Bonferroni correction for multiple testing. These four SNPs are located in *RYR2* (rs2485558, replication stage $P = 0.01$, combined $P = 1.53 \times 10^{-5}$), *DPP6* (rs916514, replication stage $P = 0.0496$, combined $P = 6.03 \times 10^{-4}$), *MMP27* (rs1939015, replication stage $P = 0.026$, combined $P = 7.09 \times 10^{-4}$) and 31 kb downstream of *NF κ BIA* (rs2145623, replication stage $P = 2.29 \times 10^{-3}$, combined $P = 5.01 \times 10^{-6}$), respectively (Table 1).

We also confirmed the previously reported association of PsV and the *LCE3C-LCE3B* deletion¹⁴ at $P = 3.80 \times 10^{-5}$ (for details on genotyping and copy number analyses, see Online Methods).

To further validate the newly associated PsV susceptibility gene *TRAF3IP2*, we genotyped the lead SNP, rs13210247, in the two

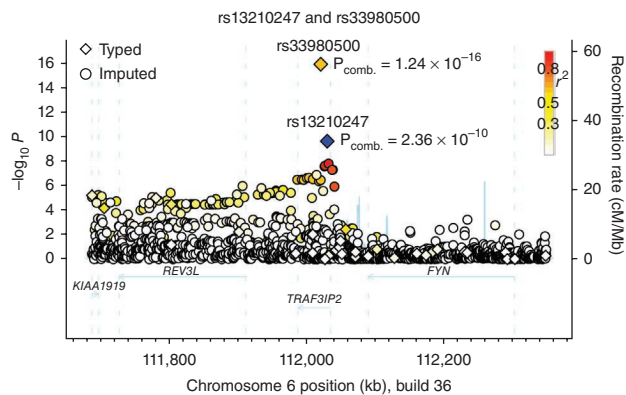


Figure 1 Regional plot of *TRAF3IP2*. Regional plot of the negative decadic logarithm of the combined P values for the imputed panels A, C and D in an ~700-kb window around the intronic lead SNP rs13210247 (blue filled diamond) and the missense SNP rs33980500 ($r^2 = 0.63$). Panels A, C and D were imputed with CEU haplotypes generated by the 1000 Genomes Project (August 2009 release) as a reference. The strongest signal of association was confined to *TRAF3IP2*. The intronic SNP rs13210247 and the missense SNP rs33980500 were genotyped in the replication panels, and the combined P values of panels A through F are indicated for both SNPs (Table 2). The magnitude of linkage disequilibrium (LD) with the central SNP rs13210247, measured by r^2 , is reflected by the color of each SNP symbol (for color coding, see upper right corner of the plot). Recombination activity (cM/Mb) is depicted by a blue line.

additional case-control panels E (1,987 cases and 1,661 controls from Michigan) and F (1,282 cases and 1,090 controls from Canada). The combined replication panels B through F comprised 6,015 PsV cases and 6,891 healthy controls, yielding a replication P value of 1.00×10^{-7} with the same direction of effect for all five panels (combined P value for panels A through F = 2.36×10^{-10}).

We additionally selected all validated coding SNPs within *TRAF3IP2* from the NCBI dbSNP¹⁶ build 130 (rs1043730, rs13190932 and rs33980500) for genotyping in replication panel B. Of the existing three missense SNPs, only rs33980500, located in exon 2, showed a significant association ($P = 0.0265$, OR = 1.28, 95% CI 1.03–1.58). Therefore, we also genotyped this SNP in the replication panels C through F. Association analysis of the obtained replication cohort (panel B through F) yielded a highly significant P value of 8.00×10^{-14} (combined P value for panels A through F = 1.24×10^{-16}) (Table 2). Because the missense SNP was not available from the HapMap II CEU imputation reference, we performed imputation based on CEU haplotypes generated by the 1000 Genomes Project for panels A, C and D in order to fine map a region of 700 kb around *TRAF3IP2* containing 1,935 SNPs (Fig. 1). The intronic *TRAF3IP2* SNP rs13210247 and the missense SNP rs33980500 are about 9.5 kb apart and are in moderate LD (LD in panels A to F, $r^2 = 0.63$). We performed a logistic regression analysis to test for the independence of these two markers. When conditioning for the missense SNP rs33980500, the intronic SNP rs13210247 was not significantly associated with disease ($P = 0.709$). In the reverse comparison, the missense SNP rs33980500 remained significantly associated ($P = 3.77 \times 10^{-7}$), indicating that it can account for the association at the *TRAF3IP2* gene locus. In a subset of German cases and controls (993 cases and 2,277 controls from panels A and B) for which HLA-Cw6 status was available, we tested for the presence of a statistical interaction between HLA-Cw6 carrier status and rs33980500 genotypes but found no statistical support for interaction ($P = 0.77$).

The missense SNP rs33980500 (Asp19Asn) causes a mutation from aspartic acid to asparagine in the protein sequence and the resulting

Table 1 Summary of association results

Chr. Position (bp)	dbSNP ID	Nearby genes (relative position)	Panel A – GWAS						Panel B		Panel C		Panel D		Panels B–D (replication only)		Panels A–D (GWAS & replication)	
			Germany						Germany		CASP		Genizon		Combined analysis		Combined analysis	
			472 cases						681 cases		1,303 cases		762 cases		2,746 cases		3,218 cases	
			1,146 controls						1,824 controls		1,322 controls		994 controls		4,140 controls		5,286 controls	
			A1 A2	AF _{A1} case	AF _{A1} control	<i>P</i>	OR (95% CI)	AF _{A1} case	AF _{A1} control	AF _{A1} case	AF _{A1} control	AF _{A1} case	AF _{A1} control	<i>P</i> _{repl.}	<i>P</i> _{comb.}			
5	rs2546890	<i>IL12B</i> (–2.5 kb)	G A	0.36	0.46	8.83×10^{-8}	0.65 (0.56–0.76)	0.38	0.44	0.42	0.49	0.45	0.53	9.07×10^{-15}	1.29×10^{-20}			
1	rs2485558	<i>RYR2</i> (intronic)	G C	0.31	0.24	2.81×10^{-6}	1.49 (1.26–1.76)	0.24	0.23	0.23	0.21	0.26	0.24	0.01	1.53×10^{-5}			
5	rs953861	<i>IL12B</i> (–15 kb)	G A	0.23	0.17	1.60×10^{-5}	1.51 (1.25–1.82)	0.22	0.18	0.22	0.17	0.21	0.14	6.50×10^{-14}	6.21×10^{-18}			
14	rs2145623	<i>NFKBIA</i> (+31 kb)	C G	0.34	0.27	3.01×10^{-5}	1.41 (1.2–1.66)	0.33	0.30	0.30	0.28	0.28	0.26	2.29×10^{-3}	5.01×10^{-6}			
6	rs13210247	<i>TRAF3IP2</i> (intronic)	G A	0.10	0.06	8.17×10^{-5}	1.7 (1.3–2.22)	0.09	0.07	0.09	0.07	0.09	0.07	6.25×10^{-6}	7.31×10^{-9}			
7	rs916514	<i>DPP6</i> (intronic)	G A	0.09	0.14	1.37×10^{-4}	0.61 (0.47–0.79)	0.09	0.11	0.09	0.11	0.10	0.09	0.0496	6.03×10^{-4}			
11	rs1939015	<i>MMP27</i> (missense)	G A	0.12	0.16	1.56×10^{-3}	0.69 (0.55–0.87)	0.14	0.14	0.15	0.17	0.17	0.20	0.026	7.09×10^{-4}			

We analyzed the top 147 SNPs of the GWAS (including typed and imputed genotypes) in three independent PsV case-control panels (B through D). Data is shown for the seven SNPs that were nominal significant in the combined replication analysis of panels B through D (replication stage $P < 0.05$, highlighted in bold) with consistent direction of effects in panels A and B. The number of cases and controls in each panel are shown in the top column. Results of all 147 SNPs are shown in **Supplementary Table 2**. SNPs are ranked according to their *P* value obtained in the GWAS. Nucleotide positions refer to NCBI build 36. Chr., chromosome. A1 denotes the minor allele and A2 is the common allele. Allele frequencies of A1 are shown (AF_{A1}). The *P* value, the odds ratio (OR) and the 95% CI for carriership of the minor allele A1 are shown for the genome-wide association analysis (panel A). The combined *P* value of the meta-analysis is shown for the independent replication panels B through D (*P*_{repl.}) as well as for the GWAS panel together with the independent replication panels (panels A through D; *P*_{comb.}). rs13210247 was additionally tested in replication panels E and F. Results for this SNP in panels B through F (replication: 6,015 cases and 6,891 controls) and panels A through F (GWAS and replication: 6,487 cases and 8,037 controls) are provided in the main text and in **Table 2**.

change in charge (a negative electric charge to nonpolar) might have an impact on the protein structure and, hence, its function. Additionally, the mutation is located in a region that is more than 90% conserved among different species (**Supplementary Fig. 3**), which further implies a possible functional consequence of this change.

Furthermore, we performed *in silico* analyses and found a putative TRAF6-binding peptide (amino acids 13 to 21) containing the SNP Asp19Asn. This peptide is similar to a known TRAF6-binding motif of CD40, a member of the tumor necrosis factor receptor superfamily¹⁷. Notably, the mutation of the accordant seventh peptide residue (asparagine to aspartate) has previously been observed to change the binding affinity of TRAF6 to CD40 significantly¹⁸. Therefore, rs33980500 may also affect the interaction of TRAF3IP2 to TRAFs and, thus, the involved inflammatory pathways.

About 15% of individuals with psoriasis develop psoriatic arthritis (PsA), which is an inflammatory, disabling arthritis^{2,19}. This suggests that PsV and PsA share common susceptibility factors.

To determine the association of the *TRAF3IP2* missense SNP with PsA, we performed a PsA stratified analysis of panels A through F. Association analysis of all individuals with PsA and controls within our combined sample (1,919 cases and 8,037 controls) yielded a *P* value of 4.57×10^{-12} for rs33980500 (OR = 1.57, 95% CI 1.38–1.78). In an equally sized subgroup of randomly extracted PsV cases without PsA, we obtained a *P* value of 2.04×10^{-6} (OR = 1.37, 95% CI 1.20–1.57). The overlap in confidence intervals for the two associations, along with the fact that no significant difference was obtained when comparing the 1,919 PsA cases versus the randomly selected 1,919 PsV cases suggests that the *TRAF3IP2* gene locus represents a shared susceptibility locus for PsA and PsV.

Gene expression of psoriatic and unaffected skin differs significantly for hundreds of genes that are involved in immune response or in the regulation of cellular differentiation and proliferation²⁰. To check if altered gene activity might trigger disease progression, we examined expression levels of several loci in biopsies from 57

Table 2 Summary of association results for the two TRAF3IP2 SNPs genotyped in additional replication panels

Chr. position (bp)	dbSNP ID	Nearby genes (relative position)	Panel A		Panel B		Panel C		Panel D		Panel E		Panel F		Panels B–F (replication only)		Panels A–F (GWAS & replication)	
			Germany		Germany		CASP		Genizon		Michigan		Canada		Combined analysis		Combined analysis	
			472 cases		681 cases		1,303 cases		762 cases		1,987 cases		1,282 cases		6,015 cases		6,487 cases	
			1,146 controls		1,824 controls		1,322 controls		994 controls		1,661 controls		1,090 controls		6,891 controls		8,037 controls	
			A1 A2	AF _{A1} case	AF _{A1} control	AF _{A1} case	AF _{A1} control	AF _{A1} case	AF _{A1} control	AF _{A1} case	AF _{A1} control	AF _{A1} case	AF _{A1} control	<i>P</i> _{repl.}	<i>P</i> _{comb.}			
6	rs13210247	<i>TRAF3IP2</i> (intronic)	G A	0.10	0.06	0.09	0.07	0.09	0.07	0.09	0.07	0.09	0.07	1.00×10^{-7}	2.36×10^{-10}			
6	rs33980500	<i>TRAF3IP2</i> (missense)	T C	0.10	0.06	0.10	0.08	0.11	0.07	0.09	0.06	0.11	0.08	8.00×10^{-14}	1.24×10^{-16}			

The lead SNP rs13210247 and the missense SNP rs33980500 were genotyped in five independent PsV case-control panels (B through F; **Supplementary Table 1**). The number of cases and controls of each panel is shown in the top column. Nucleotide positions refer to NCBI build 36. Chr., chromosome. A1 denotes the rare allele and A2 is the common allele. Allele frequencies of A1 are shown (AF_{A1}). The combined *P* value of the meta-analysis is shown for the independent replication panels B to F (*P*_{repl.}) as well as for the GWAS panel together with the independent replication panels (panels A through F; *P*_{comb.}).

healthy controls and compared these to expression levels of biopsies of involved and uninvolved skin from 53 PsV cases (subgroup of panel C). We analyzed the *TRAF3IP2* locus and some genes that potentially act downstream of *TRAF3IP2*. For the *TRAF3IP2* locus, the expression level was slightly altered between involved and uninvolved skin ($P = 2.2 \times 10^{-3}$) (Supplementary Fig. 4). However, the dosage of risk alleles at the according SNPs did not correlate with transcript levels for the genes in involved, uninvolved or normal skin (Supplementary Table 3).

Genetic variants in the *TRAF3IP2* locus are implicated in PsV and PsA susceptibility for the first time, to our knowledge, by our study. The gene product of *TRAF3IP2* is a positive signaling adaptor required for IL-17-mediated T-cell immune responses²¹. TRAF3IP2 interacts with tumor necrosis factor receptor-associated factor (TRAF) proteins and either I- κ B kinase or mitogen-activated protein kinase to activate either NF- κ B or Jun kinase. Upon recruitment to CD40 and the BAFF receptor in B cells, TRAF3IP2 also negatively regulates B-cell survival through its interaction with TRAF3 (ref. 22). The negative regulation of CD40-BAFF-mediated B-cell functions results in 'hyper-T-cell-dependent' and T-cell-independent immune responses in TRAF3IP2-deficient mice. Researchers in a previous study also found that TRAF3IP2 is a key component of IL-17-mediated signaling and that IL-17-mediated gene expression is completely abolished in TRAF3IP2-deficient mouse embryonic fibroblasts. In addition, epithelial cells have been identified as the critical cell type in which TRAF3IP2 mediates IL-17-dependent inflammatory disease²¹. In PsV, a subset of T cells expressing IL-17 plays a major role²³. The IL-17-expressing T cells that are abundant in the epidermis of psoriatic lesions but which are absent in healthy donor epidermis are CD8+ cells, whereas in lesional psoriatic dermis, mainly IL-17-expressing CD4+ (but also CD8+) T cells are strongly increased relative to healthy skin. Epidermal hyperplasia and the production of innate immune peptides such as human β -defensin 2 (hBD-2) are associated with these IL-17+ T cells²⁴. The crucial role of IL-17 is also supported by the observation that in psoriasis, treatment response to TNF inhibitors correlates with suppressed IL-17 signaling²⁵. Moreover, we showed that in immortalized N-TERT keratinocytes (N-TERT KCs) and in normal human keratinocytes (NHKs), IL-17A and TNF- α together induce the expression of *DEFB4* (encoding hBD-2), which is absent in N-TERT KCs and NHKs with silenced *TRAF3IP2* (Supplementary Fig. 5). In epithelial cells, the binding of IL-17A and/or IL-17F to the heterodimeric IL-17R leads to the recruitment of TRAF3IP2 through homotypic interactions between conserved (SEFIR) domains. This allows the incorporation of TRAF6 into the signaling complex followed by downstream activation of the NF- κ B and mitogen-activated protein kinase pathways²⁶. We thus speculate that a dysregulation of TRAF3IP2 might have a major impact on IL-17 signaling and, hence, on the activation of NF κ B-pathways, leading to the upregulation of pro-inflammatory factors.

For the *TRAF3IP2* locus newly identified here, fine mapping and resequencing efforts together with extensive functional studies are required to detect all potential causal variants and thus to specify the contribution of the locus to overall disease susceptibility.

URLs. METAL software, <http://www.sph.umich.edu/csg/abecasis/Metal/>; dbGAP, <http://www.ncbi.nlm.nih.gov/gap/>; NGFN Funding, press release 04-26-2007, http://www.ngfn.de/en/index_368.htm or <http://idw-online.de/pages/en/news206267>; MACH and MACH2DAT software, <http://www.sph.umich.edu/csg/abecasis/mach/>; HapMap data, http://hapmap.ncbi.nlm.nih.gov/downloads/phasing/2006-07_phaseII/phased/; PLINK v1.05, <http://pngu.mgh.harvard.edu/~purcell/plink/>; R statistical environment version 2.10.0, <http://www.r-project.org/>.

METHODS

Methods and any associated references are available in the online version of the paper at <http://www.nature.com/naturegenetics/>.

Accession codes. The CASP GWAS dataset (panel C) is deposited in dbGaP under the accession code phs000019.v1.p1.

Note: Supplementary information is available on the Nature Genetics website.

ACKNOWLEDGMENTS

We thank all individuals with psoriasis who participated in this study, their families and their physicians for their cooperation. We acknowledge the cooperation of Genizon Biosciences. We wish to thank T. Wesse, T. Henke, C. Fürstenau, S. Ehlers, M. Davids and R. Vogler for expert technical help. We thank J.R. Hov for helpful discussions. This study was supported by the German Ministry of Education and Research (BMBF) through the National Genome Research Network (NGFN), the PopGen biobank and the KORA (Cooperative Research in the Region of Augsburg) research platform. KORA was initiated and financed by the Helmholtz Zentrum München-National Research Center for Environmental Health, which is funded by the German Federal Ministry of Education, Science, Research and Technology and by the State of Bavaria and the Munich Center of Health Sciences (MC Health) as part of LMUinnovativ. The project received infrastructure support through the Deutsche Forschungsgemeinschaft (DFG) clusters of excellence 'Multimodal Computing and Interaction' and 'Inflammation at Interfaces'. This research was also supported by grants R01-AR42742, R01-AR050511 and R01-AR054966 from the US National Institutes of Health.

AUTHOR CONTRIBUTIONS

E.E. performed SNP selection, genotyping, data analysis and prepared the figures and tables. A.F. helped with data analysis. D.E. performed imputation, data analysis and generated the regional plots. P.E.S., J.G., J.D. and Y.L. performed the expression and expression quantitative trait loci analyses. S.W.S. and S.L. performed small hairpin RNA (shRNA) experiments. G.R.A. helped with statistical analyses and interpretation of the results. M.A. and G.M. performed *in silico* protein analyses. M.W., U.M., S.W., B.E. and M.K. coordinated the recruitment and collected phenotype data of panels A and B. C.G. and H.E.W. provided the KORA control samples. J.T.E., J.J.V., R.P.N., T.T., S.D., J.V.R., M.B., H.F., C.R., P.R. and D.D.G. provided the replication samples C through F and the respective genotypes and phenotypes. T.H.K., R.P.N. and D.K. helped with genotyping. E.E. and A.F. drafted the manuscript. D.E., M.W., J.T.E., T.H.K. and S.S. edited the manuscript. A.F. planned and supervised the study. All authors approved the final draft.

COMPETING FINANCIAL INTERESTS

The authors declare no competing financial interests.

Published online at <http://www.nature.com/naturegenetics/>.

Reprints and permissions information is available online at <http://npg.nature.com/reprintsandpermissions/>.

- Griffiths, C.E. & Barker, J.N. Pathogenesis and clinical features of psoriasis. *Lancet* **370**, 263–271 (2007).
- Bowcock, A.M. & Barker, J.N. Genetics of psoriasis: the potential impact on new therapies. *J. Am. Acad. Dermatol.* **49**, S51–S56 (2003).
- Gottlieb, A.B. Psoriasis: emerging therapeutic strategies. *Nat. Rev. Drug Discov.* **4**, 19–34 (2005).
- Oudot, T. *et al.* An association study of 22 candidate genes in psoriasis families reveals shared genetic factors with other autoimmune and skin disorders. *J. Invest. Dermatol.* **129**, 2637–2645 (2009).
- Bhalerao, J. & Bowcock, A.M. The genetics of psoriasis: a complex disorder of the skin and immune system. *Hum. Mol. Genet.* **7**, 1537–1545 (1998).
- Elder, J.T. *et al.* The genetics of psoriasis. *Arch. Dermatol.* **130**, 216–224 (1994).
- Tsunemi, Y. *et al.* Interleukin-12 p40 gene (IL12B) 3-untranslated region polymorphism is associated with susceptibility to atopic dermatitis and psoriasis vulgaris. *J. Dermatol. Sci.* **30**, 161–166 (2002).
- Cargill, M. *et al.* A large-scale genetic association study confirms IL12B and leads to the identification of IL23R as psoriasis-risk genes. *Am. J. Hum. Genet.* **80**, 273–290 (2007).
- Capon, F. *et al.* Sequence variants in the genes for the interleukin-23 receptor (IL23R) and its ligand (IL12B) confer protection against psoriasis. *Hum. Genet.* **122**, 201–206 (2007).
- Nair, R.P. *et al.* Polymorphisms of the IL12B and IL23R genes are associated with psoriasis. *J. Invest. Dermatol.* **128**, 1653–1661 (2008).
- Liu, Y. *et al.* A genome-wide association study of psoriasis and psoriatic arthritis identifies new disease loci. *PLoS Genet.* **4**, e1000041 (2008).
- Chang, M. *et al.* Variants in the 5q31 cytokine gene cluster are associated with psoriasis. *Genes Immun.* **9**, 176–181 (2008).

13. Nair, R.P. *et al.* Genome-wide scan reveals association of psoriasis with IL-23 and NF-kappaB pathways. *Nat. Genet.* **41**, 199–204 (2009).
14. de Cid, R. *et al.* Deletion of the late cornified envelope *LCE3B* and *LCE3C* genes as a susceptibility factor for psoriasis. *Nat. Genet.* **41**, 211–215 (2009).
15. Zhang, X.J. *et al.* Polymorphisms in interleukin-15 gene on chromosome 4q31.2 are associated with psoriasis vulgaris in Chinese population. *J. Invest. Dermatol.* **127**, 2544–2551 (2007).
16. Sherry, S.T. *et al.* dbSNP: the NCBI database of genetic variation. *Nucleic Acids Res.* **29**, 308–311 (2001).
17. Ye, H. *et al.* Distinct molecular mechanism for initiating TRAF6 signalling. *Nature* **418**, 443–447 (2002).
18. Darnay, B.G., Ni, J., Moore, P.A. & Aggarwal, B.B. Activation of NF-kappaB by RANK requires tumor necrosis factor receptor-associated factor (TRAF) 6 and NF-kappaB-inducing kinase. Identification of a novel TRAF6 interaction motif. *J. Biol. Chem.* **274**, 7724–7731 (1999).
19. Gelfand, J.M. *et al.* Epidemiology of psoriatic arthritis in the population of the United States. *J. Am. Acad. Dermatol.* **53**, 573 (2005).
20. Zhou, X. *et al.* Novel mechanisms of T-cell and dendritic cell activation revealed by profiling of psoriasis on the 63,100-element oligonucleotide array. *Physiol. Genomics* **13**, 69–78 (2003).
21. Qian, Y. *et al.* The adaptor Act1 is required for interleukin 17-dependent signaling associated with autoimmune and inflammatory disease. *Nat. Immunol.* **8**, 247–256 (2007).
22. Qian, Y. *et al.* Act1, a negative regulator in CD40- and BAFF-mediated B cell survival. *Immunity* **21**, 575–587 (2004).
23. Lowes, M.A. *et al.* Psoriasis vulgaris lesions contain discrete populations of Th1 and Th17 T cells. *J. Invest. Dermatol.* **128**, 1207–1211 (2008).
24. Kryczek, I. *et al.* Induction of IL-17+ T cell trafficking and development by IFN- γ : mechanism and pathological relevance in psoriasis. *J. Immunol.* **181**, 4733–4741 (2008).
25. Zaba, L.C. *et al.* Effective treatment of psoriasis with etanercept is linked to suppression of IL-17 signaling, not immediate response TNF genes. *J. Allergy Clin. Immunol.* **124**, 1022–10 e1–395 (2009).
26. Hunter, C.A. Act1-ivating IL-17 inflammation. *Nat. Immunol.* **8**, 232–234 (2007).

ONLINE METHODS

Recruitment of cases and controls. Samples were organized in panels that corresponded to the successive steps of the present study. All individual panels (A–F) were independent from each other.

All German cases in panels A and B were recruited either at the Department of Dermatology of the Christian-Albrechts-University Kiel or the Department of Dermatology and Allergy of the Technical University Munich through local outpatient services. Individuals were considered to be affected if chronic plaque or guttate psoriasis lesions covered more than 1% of their total body surface area or if at least two skin, scalp, nail or joint lesions were clinically diagnosed as being caused by psoriasis. Psoriatic arthritis (PsA) was diagnosed by a clinical finding of joint complaints and radiologic and rheumatologic confirmation by criteria according to Moll and Wright²⁷, or more recently, to the Classification Criteria for Psoriatic Arthritis (CASPAR)²⁸.

2,510 German healthy control individuals in panels A and B were obtained from the PopGen biobank²⁹. 483 German healthy controls were selected from the KORA S4 survey, an independent population-based sample from the general population living in the region of Augsburg, southern Germany³⁰.

The American study population (panel C) consisted of 1,303 psoriasis cases and 1,322 controls after quality control measures. The datasets used for the analyses described in this manuscript were obtained from the database of Genotype and Phenotype (dbGaP). The genotyping of samples was provided through the Genetic Association Information Network (GAIN). Samples and associated phenotype data were provided by the Collaborative Association Study of Psoriasis (CASP). Funding support for CASP was provided by the US National Institutes of Health, the Foundation for NIH's Genetic Association Information Network and the National Psoriasis Foundation.

The Canadian population sample used for panel D consisted of 762 psoriasis cases and 994 controls sampled from the Québec founder population (QFP). Membership in the QFP was defined as having four grandparents with French-Canadian family names who were born in the Province of Québec, Canada or in adjacent areas in the provinces of New Brunswick and Ontario or in New England or New York State. This criterion assured that all subjects were descendants of French-Canadians living before the 1960s, after which time admixture with non-French-Canadians became more common.

For replication of the two *TRAF3IP2* SNPs (rs13210247 and rs33980500), panel E was tested for an association. This panel comprised 1,987 psoriasis cases and 1,661 controls of European ancestry. The sample was collected at the University of Michigan, and selection criteria for cases included a requirement of at least two psoriatic plaques or a single plaque occupying >1% of an individual's total body surface area outside the scalp. Individuals that presented only palmoplantar psoriasis, inverse psoriasis or seborrheic psoriasis were excluded. Individuals used as controls were older than 18 years and had no history of psoriasis and no family history of psoriasis.

Panel F, also used only for replication of the two *TRAF3IP2* SNPs, consisted of 1,282 psoriasis cases and 1,090 controls from Toronto and Newfoundland, Canada. Psoriasis was diagnosed by a dermatologist. Control individuals showed no evidence of psoriasis, rheumatoid arthritis or other autoimmune disorders.

Written, informed consent was obtained from all study participants, and all protocols were approved by the respective institutional ethical review committees of the participating centers.

SNP genotyping for the genome-wide screen. The genotyping for the GWAS, which was part of the German GWAS initiative funded by the National Genome Research Network (NGFN), was performed by Illumina's service facility using the Illumina HumanHap 550K v1 with 561,466 SNP markers. All experimental steps were carried out according to standard protocols.

We excluded five samples with more than 10% missing genotypes (that is, having a call rate <90%). Individuals who showed statistically relevant genetic dissimilarity to the other subjects (population outliers) or who showed evidence for cryptic relatedness to other study participants (unexpected duplicates, first- or second-degree relatives) were removed (Supplementary Fig. 1). These quality control measures left 472 psoriasis samples and 1,146 control samples for inclusion in screening panel A. All gender assignments could be verified by reference to the proportion of heterozygous SNPs on the X chromosome. Before analysis, we excluded 56,724 markers (10% of the total number of SNPs) that had a low genotype call rate (<95% in cases or controls; $n = 4,254$), were monomorphic or

rare (minor allele frequency <2% in cases or controls; $n = 30,862$), deviated from Hardy-Weinberg equilibrium (HWE) in the control sample (HWE $P < 0.01$; $n = 7,600$) or that were nonautosomal SNPs ($n = 14,008$).

Imputation. Genotype imputation was performed using a hidden Markov model algorithm implemented in the software program MACH v.1.0.16³¹ to infer missing genotypes *in silico*. As a reference, HapMap II CEU phased haplotypes³² were used.

As input for the imputation, only genotyped SNPs that passed quality control were used. Of the imputed SNPs, we analyzed only those SNPs that could be imputed with a relatively high confidence (estimated r^2 between imputed SNP and true genotypes >0.3), had a minor allele frequency >2% in cases or controls and a HWE P value < 0.01 in the control sample. To take imputation uncertainty into account, we used allelic dosage association as implemented in the program MACH2DAT³¹. The allelic dosage is the weighted sum of the genotype class probabilities.

SNP selection for replication. SNPs in the genome-wide scan that passed quality control were analyzed using gPLINK v2.049 in combination with PLINK v1.05³³. The SNP list (including imputed and genotyped SNPs) was pruned for redundancy due to linkage disequilibrium by using the `-clump` command in PLINK. For all genotyped index SNPs with $P < 10^{-3}$, a visual inspection of the cluster plots was performed. SNPs that did not pass the visual inspection were excluded from further analyses. The 180 most strongly associated index SNPs of the clumps ($P < 2.6 \times 10^{-4}$) were ordered as genotyping assays. If the genotyping assay design was not possible for a SNP, the next best SNP from the clump was chosen for the assay design.

SNPlex and TaqMan genotyping. The ligation-based SNPlex genotyping system and functionally tested TaqMan SNP Genotyping Assays (Applied Biosystems) were used to genotype variants in replication panel B. For technical replication of the results of the two *TRAF3IP2* SNPs, TaqMan SNP Genotyping Assays were used in panels A–E and the Sequenom Platform was used for panel F.

Of the 180 selected SNPs, 147 SNPs passed quality control measures. These SNPs had a high call rate (>90% in cases or controls; 25 SNPs were removed), were not monomorphic (minor allele frequency >1% in cases or controls; 2 SNPs were removed) and did not deviate from Hardy-Weinberg equilibrium in the control population (HWE $P > 0.0001$; 5 SNPs were removed). One SNP failed genotyping and was excluded from the analysis.

Copy number variation genotyping and quality control. The functionally tested TaqMan Copy Number Assays Hs 02550639_cn (for *LCE3C*) and Hs 02878369_cn (for *LCE3B*) (Applied Biosystems) were used to genotype copy number variation within the *LCE* gene cluster in samples of panel A and B (754 cases and 1,052 controls). Genotyping was carried out according to Applied Biosystems' standard protocols with 5 ng of dried DNA per well.

All cases were genotyped three times and all control samples were genotyped four times. The generated data was analyzed with the analysis software CopyCaller v1.0. The analysis settings were selected as recommended by the CopyCaller software user guide. The chosen confidence threshold of the associated predicted copy number was $\geq 95\%$. Control samples were removed when more than one of the four measurements did not pass quality control measures, whereas cases were removed when one of the three measurements did not pass quality control. Altogether, 736 cases and 932 controls remained for association analysis (94% of all samples).

Statistical analyses. Power calculations were carried out using PS Power and Sample Size v3.0.12³⁴. GWAS data were analyzed using R statistical environment version 2.10.0 and gPLINK v2.049 in combination with PLINK v1.05³³. The `-clump` command was used to reduce the number of SNPs for follow-up by removing correlated hit SNPs. The meta-analysis of the different panels was performed with METAL³⁵.

TRAF3IP2 silencing in keratinocytes. Small hairpin RNA (shRNA) targeting enhanced green fluorescent protein (EGFP) was cloned into the pLenti4/Block-iT-DEST (Invitrogen) as previously described³⁶. shRNA lentiviral

constructs directed against *TRAF3IP2* were obtained from Sigma. Lentiviral particles were produced in 293FT cells and used to infect immortalized N-TERT keratinocytes (kindly provided by J. Rheinwald) and normal human keratinocytes (NHK) at 10–20% confluence as previously described³⁷. After 72 h of infection, the cells were incubated in basal medium and stimulated for 30 h with IL17 (10 ng/ml), IL22 (10 ng/ml) and/or TNF- α (20 ng/ml). Total RNA was isolated using RNeasy Mini Kits with on-column DNase digestion according to the manufacturer's instructions (Qiagen) and were reverse transcribed using the High Capacity cDNA Reverse Transcription Kit (Applied Biosystems). Real-time PCR analysis for *DEFB4*, *TRAF3IP2* and the control gene *RPLP0* (encoding ribosomal protein P0) was performed using prevalidated TaqMan gene expression assays from Applied Biosystems according to the manufacturer's instructions. Target gene expression was normalized to the control gene *RPLP0*, and mRNA levels were expressed as a percent of *RPLP0*.

27. Moll, J.M. & Wright, V. Psoriatic arthritis. *Semin. Arthritis Rheum.* **3**, 55–78 (1973).
28. Taylor, W. *et al.* Classification criteria for psoriatic arthritis: development of new criteria from a large international study. *Arthritis Rheum.* **54**, 2665–2673 (2006).
29. Krawczak, M. *et al.* PopGen: population-based recruitment of patients and controls for the analysis of complex genotype-phenotype relationships. *Community Genet.* **9**, 55–61 (2006).
30. Wichmann, H.E., Gieger, C. & Illig, T. KORA-gen—resource for population genetics, controls and a broad spectrum of disease phenotypes. *Gesundheitswesen* **67** Suppl 1, S26–S30 (2005).
31. Li, Y., Willer, C., Sanna, S. & Abecasis, G. Genotype imputation. *Annu. Rev. Genomics Hum. Genet.* **10**, 387–406 (2009).
32. The International HapMap Consortium. *et al.* A second generation human haplotype map of over 3.1 million SNPs. *Nature* **449**, 851–861 (2007).
33. Purcell, S. *et al.* PLINK: a tool set for whole-genome association and population-based linkage analyses. *Am. J. Hum. Genet.* **81**, 559–575 (2007).
34. Dupont, W.D. & Plummer, W.D. PS power and sample size program available for free on the Internet. *Control. Clin. Trials* **18** (1997).
35. Willer, C.J., Li, Y. & Abecasis, G.R. METAL: fast and efficient meta-analysis of genomewide association scans. *Bioinformatics* **26**, 2190–2191 (2010).
36. Stoll, S.W., Johnson, J.L., Li, Y., Rittie, L. & Elder, J.T. Amphiregulin carboxy-terminal domain is required for autocrine keratinocyte growth. *J. Invest. Dermatol.* **130**, 2031–2040 (2010).
37. Stoll, S.W. *et al.* Metalloproteinase-mediated, context-dependent function of amphiregulin and HB-EGF in human keratinocytes and skin. *J. Invest. Dermatol.* **130**, 295–304 (2010).

